# Stability of Perpendicular and Parallel Lamellae within Lamellae of Multiblock Terpolymers†

**Yuci Xu, Weihua Li,* Feng Qiu, and Yuliang Yang**

*The Key Laboratory of Molecular Engineering of Polymers, Ministry of Education, China, and Department of Macromolecular Science, Fudan University, Shanghai 200433, China*

**An-Chang Shi**

*Department of Physics and Astronomy, McMaster University, Hamilton, Ontario, Canada, L8S 4M1*

*Received: July 22, 2010; Revised Manuscript Received: September 27, 2010*

The phase behaviors of multiblock terpolymer $A(BC)_nB$ (or $A(BC)_n$) with equal volume fractions of A and compositional symmetric $(BC)_nB$ (or $(BC)_n$) are investigated by using the pseudospectral method of the self-consistent mean field theory. These terpolymers can self-assemble into hierarchical lamellar phases of perpendicular or parallel lamellae within lamellae, and the number of B/C thin layers in the parallel phase can be varied. The relative stability among these hierarchical lamellar phases can be tuned by the three interaction parameters of $\chi_{AB}N$, $\chi_{AC}N$, and $\chi_{BC}N$. Two-dimensional phase diagrams, the cross sections of the three-dimensional phase diagram, are determined in our calculations. Our conclusion that the perpendicular phase is stable only in the case of $\chi_{AC}N \ll \chi_{AB}N < \chi_{BC}N$ is consistent with experimental observations by Bates's group. In addition, our results suggest that the existence of the perpendicular phase is generic in both types of terpolymers: $A(BC)_nB$ and $A(BC)_n$, with different values of $n$, even for the special case of $A(BC)_n$, that is, an ABC linear terpolymer.

## I. Introduction

Block copolymers have received abiding attention because of their ability to self-assemble into a variety of ordered nanoscale structures. These nanostructures possess great potential for applications in the fabrication of functional materials including lithographic templates for quantum dots,[1] nanowires,[2] high density magnetic storage media,[3] and silicon capacitors.[4] As the simplest model of block copolymers, the diblock copolymer has been extensively studied both experimentally and theoretically, and a good understanding of diblock copolymer phase behavior has been obtained. The classical mesophases formed by diblock copolymers include lamellae, cylinders, spheres, gyroid, and *Fddd* (orthorhombic network) phases with length scales on the order of 10−100 nm.[5−7] Most of those periodically ordered structures usually involve only one characteristic length scale which may limit their application in manufacturing functional materials. By introducing a new component into AB diblock copolymers, ABC terpolymers with various architectures can be synthesized. For the ABC triblock copolymers, there are two kinds of topologies: linear and star. Much more mesophases beyond those formed in diblock copolymers have been observed in ABC triblock copolymers.[8−14] It has emerged from these previous studies that the ABC terpolymers provide a platform to explore new structures which may contain different length scales by varying the number of blocks and controlling the architectures.

The first observation of hierarchical structures with two length scales from a block copolymer system was reported by ten Brinkes and co-workers using comb-shaped supramolecules consisting of polystyrene-block-poly(4-vinylpyridine) (PS-b-P4VP) diblock copolymers and pentadecylphenol (PDP) which can be attached to the P4VP blocks via a hydrogen bond.[15,16] In the observed hierarchical lamellae, the P4VP(MSA)PDP and PS form alternating layers with a long period, and the P4VP(MSA)-PDP layers are further microphase-separated into sublayers with a short period, which are aligned normal to the major layers. Because the PDP molecules are attached to the sulfonate groups of P4VP(MSA) by hydrogen-bond interactions, the microphase separation between P4VP(MSA) and PDP is sensitive to the temperature. Increasing the temperature can result in the order−order transition that the hierarchical lamellar structure becomes simple lamellae. In a subsequent work, Ruokolainen et al. observed more hierarchical structures, including lamellae within lamellae, lamellae within cylinders, cylinders within lamellae, spheres within lamellae, and lamellae within spheres, with a simpler supramolecule of PS-b-P4VP-(PDP).[17] Besides the supramolecule made by using hydrogen-bond interactions, complex block copolymers can be used to fabricate a variety of hierarchical structures.

One example of hierarchical block copolymer phases is found in an undecablock terpolymer synthesized by Matsushita and co-workers,[18,19] which exhibits hierarchical lamellae of parallel lamellae in lamellae. This new type of linear multiblock (PISISISISIP) terpolymer consists of two long poly(2-vinylpyridine) (P) blocks on each end and five short polyisoprene (I) plus four short polystyrene (S) blocks in the middle. The self-assembled lamellae are composed of alternative thick layers of P-blocks and thin layers of B/C blocks. The number of thin B/C layers within lamella is largely, although not exclusively, determined by the number of B/C blocks. A geometric model, based on counting possible configurational paths of the terpolymer, was proposed by Matsushita et al. to explain the dependence of the

† PACS numbers: 61.25.Hq, 64.60.Cn, 64.75.+g.

* Corresponding author. E-mail: weihuali@fudan.edu.cn.

10.1021/jp1068335 
Published on Web 10/28/2010

number of midlayers on the B/C blocks. This simple model gives a qualitative prediction of number of thin B/C layers, but it only considers the entropic contribution and ignores the interfacial energy. In a subsequent study, Li and Shi systematically investigated the self-assemblies of $A(BC)_nBA$ terpolymers by means of the real-space calculations of the self-consistent mean-field theory (SCMFT).[20] Their results demonstrated that more than one of the hierarchical lamellar phases with a different number of thin B/C midlayers can be stable for a given $A(BC)_nBA$ terpolymer, and their relative stability can be tuned by the three interactions of $\chi_{AB}N$, $\chi_{AC}N$, and $\chi_{BC}N$. This prediction is very consistent with those of the strong-segregation theory (SST) and the dissipative particle dynamic (DPD) simulations by ten Brinke et al.[21] More recently, the formation of hierarchical phases has attracted increasing interest. A number of linear multiblock copolymers such as $A(BA)_nBA$, $A(BA)_n$, and $A(BC)_nBA$, have been studied by SCMFT[22−24] and SST.[25,26] In these multiblock copolymers, the most studied hierarchical lamellar phase is of the type of parallel lamellae in lamellae, and the formation of the perpendicular lamellae in lamellae phases is rarely examined.

Very recently, Fleury and Bates have synthesized a monodisperse poly(CECEC-P) (C: cyclohexylethylene, E: ethylene, P: propylene) hexablock terpolymer by sequential anionic polymerization followed by catalytic hydrogenation.[27,28] The linear multiblock terpolymer consists of equal amounts of E(25%) and C(25%) and symmetric volume fractions of CECEC and P(50%). A perpendicular lamellae, which is composed of thin C/E sublayers arranged perpendicular to the larger layered structure, was identified. In general, the morphology formation is determined by the competition between the chain entropy and the interfacial energy. Emphasizing the interfacial energy contribution, the authors rationalized this interesting morphology based on the documented ordering of the segment−segment interaction parameters: $\chi_{CE} > \chi_{CP} \gg \chi_{EP}$. Compared with the parallel hierarchical phase, the perpendicular lamellae phase is penalized by the presence of the E/P interfaces. The small $\chi_{EP}$ value in the current system ensures that the energy penalty induced by the E/P interfaces is not high; thus, it can be compensated by the entropic gain from the arrangement of C/E domains in the perpendicular phase where it is near free from the soft confinement by P domains. This simple argument gives a qualitative understanding of the system. However, it cannot give a quantitative account for the influence of the interactions on the stability of the perpendicular phase. A systematically theoretical study is necessary for further understanding on the phase behaviors of this type of terpolymers.

Theoretically, Lin et al. has carried out a preliminary study on the self-assembling behavior of linear $A(BC)_n$ terpolymers using SCMFT.[29] They mainly focused on the exploration of the formation of novel hierarchical structures in this terpolymers. A number of hierarchical structures including perpendicular or parallel lamellae, cylinders and spheres, have been observed. Only for one example of a case with A volume fraction of 0.5 and symmetric B/C compositions, Lin et al. found that the parallel lamellar phase with five mid-B/C layers transfers to the perpendicular phase when $\chi_{BC}N$ is much larger than $\chi_{AC}N$ for fixed $\chi_{AB}N = 100$ or $\chi_{AB}N = 150$. Very recently, Subbotin et al. studied perpendicular or parallel lamellar-within-lamellar morphologies of $A(BA)_nC$ multiblock terpolymer melts at the strong segregation limit.[36] They investigated the influence of interaction parameters and the numbers of repeating AB blocks $n$ on the phase behavior. Despite these previous studies, our understanding of the relative stability of the two types of hierarchical lamellar phases formed in linear multiblock terpolymers is still incomplete.

In the present work, we focus on the relatively stability of parallel and perpendicular hierarchical lamellar phases in $A(BC)_nB$ or $A(BC)_n$ multiblock terpolymers. Specifically we focus on the influence of different factors including the three interaction parameters and the number of B/C blocks. When $n = 1$, the $A(BC)_n$ terpolymer is reduced to an ABC linear triblock copolymer. An interesting ABC linear triblock copolymer is the so-called type II frustrated one, in which $\chi_{AC}N$ is the smallest interaction among the three interactions.[8,30] In the systems with type II frustration, a number of novel decorated phases, such as spheres on spheres, spheres on cylinders, rings on cylinders, and cylinders in lamellae, can be formed.[31] Considering the condition of $f_A = 0.5$ and $f_B = f_C = 0.25$, it can predict that the perpendicular lamellar in lamellar phase might become stable as a frustrated phase. To calculate the free energy of different morphologies, we employ the real-space method of SCMFT in our study. It is known that SCMFT is a powerful theoretical framework which is capable of connecting molecular architecture and composition to equilibrium ordered phases.[32,33] In our study, solutions of SCMFT equations corresponding to hierarchical lamellar structures are obtained. A comparison of the free energy of these phases leads to the construction of phase diagrams of the copolymers. The phase diagrams reveal the stability region of different morphologies.

## II. Theory

We consider an incompressible melt of $A(BC)_nB/A(BC)_n$ multiblock terpolymers with a degree of polymerization $N$ in a volume of $V$. The chain lengths of A, B, and C blocks are $f_AN$, $f_BN$, and $f_CN$ ($f_A + f_B + f_C = 1$), respectively. The radius of gyration of the polymer, $R_g$, is used as the length unit in our calculations. Within the mean-field approximation to statistical mechanics of the Edwards model of polymers,[32,33] at a temperature $T$, the free energy functional $F$ for $n$ Gaussian triblock copolymer chains is

$$\frac{F}{nk_BT} = -\ln Q + \frac{1}{V}\int d\mathbf{r}\{\chi_{AB}N\phi_A(\mathbf{r})\phi_B(\mathbf{r}) + \chi_{AC}N\phi_A(\mathbf{r})\phi_C(\mathbf{r}) + \chi_{BC}N\phi_B(\mathbf{r})\phi_C(\mathbf{r}) - \omega_A(\mathbf{r})\phi_A(\mathbf{r}) - \omega_B(\mathbf{r})\phi_B(\mathbf{r}) - \omega_C(\mathbf{r})\phi_C(\mathbf{r}) - \eta(\mathbf{r})[1 - \phi_A(\mathbf{r}) - \phi_B(\mathbf{r}) - \phi_C(\mathbf{r})]\} \quad (1)$$

where $\phi_A$, $\phi_B$, and $\phi_C$ are the monomer densities. The partition function $Q$ is for a single polymer chain interacting with the mean fields of $\omega_A$, $\omega_B$, and $\omega_C$ produced by the surrounding chains. The interactions among the three dissimilar monomers are characterized by three Flory−Huggins interaction parameters, $\chi_{AB}$, $\chi_{AC}$, and $\chi_{BC}$. The minimization of the free energy with respect to the monomer densities and the mean fields leads to the following standard mean-field equations[32,33]

$$\begin{aligned}
\omega_A(\mathbf{r}) &= \chi_{AB}N\phi_B(\mathbf{r}) + \chi_{AC}N\phi_C(\mathbf{r}) + \eta(\mathbf{r}) \\
\omega_B(\mathbf{r}) &= \chi_{AB}N\phi_A(\mathbf{r}) + \chi_{BC}N\phi_C(\mathbf{r}) + \eta(\mathbf{r}) \\
\omega_C(\mathbf{r}) &= \chi_{AC}N\phi_A(\mathbf{r}) + \chi_{BC}N\phi_B(\mathbf{r}) + \eta(\mathbf{r}) \\
\phi_A(\mathbf{r}) &= \frac{1}{Q}\int_0^{f_A} \mathrm{d}s\, q_A(\mathbf{r}, s)q_A^\dagger(\mathbf{r}, s) \\
\phi_B(\mathbf{r}) &= \frac{1}{Q}\int_{s\in B} \mathrm{d}s\, q_B(\mathbf{r}, s)q_B^\dagger(\mathbf{r}, s) \\
\phi_C(\mathbf{r}) &= \frac{1}{Q}\int_{s\in C} \mathrm{d}s\, q_C(\mathbf{r}, s)q_C^\dagger(\mathbf{r}, s) \\
Q &= \frac{1}{V}\int \mathrm{d}\mathbf{r}\, q_K(\mathbf{r}, s)q_K^\dagger(\mathbf{r}, s) \\
\phi_A(\mathbf{r}) &+ \phi_B(\mathbf{r}) + \phi_C(\mathbf{r}) = 1
\end{aligned} \tag{2}$$

The integration in the density of $\phi_B$ or $\phi_C$ is conducted along each block of B or C. The quantities, $q_K(\mathbf{r}, s)$ and $q_K^\dagger(\mathbf{r}, s)$ (K = A, B, C) are end-segment distribution functions which have standard definitions.[32,33] These distribution functions satisfy the modified diffusion equations

$$\frac{\partial q_K(\mathbf{r}, s)}{\partial s} = \nabla^2 q_K(\mathbf{r}, s) - \omega_K(\mathbf{r}, s)q_K(\mathbf{r}, s) \tag{3}$$

$$-\frac{\partial q_K^\dagger(\mathbf{r}, s)}{\partial s} = \nabla^2 q_K^\dagger(\mathbf{r}, s) - \omega_K(\mathbf{r}, s)q_K^\dagger(\mathbf{r}, s) \tag{4}$$

The initial conditions are $q_A(\mathbf{r}, 0) = 1$ and $q_B^\dagger(\mathbf{r}, 1) = 1$ (or $q_C^\dagger(\mathbf{r}, 1) = 1$) for A(BC)$_n$B (or A(BC)$_n$). For numerical solutions, we employ the pseudospectral method[34,35] to solve the modified diffusion equations for the end-segment distribution functions. One-dimensional and two-dimensional (2D) calculations are carried for the parallel and perpendicular lamellar phases, respectively. Periodic boundary conditions are imposed automatically on each direction of the box, and the free energy is minimized with respect to the box sizes. The total chain contour is discretized into 500 points which are enough to give reliable results of phase boundaries although it cannot get high accurate free energy.[14]

## III. Results and Discussion

In the experiment of ref 27, the perpendicular lamellae in lamellae are observed in A(BC)$_2$B terpolymers with $f_A = 0.50$, and $f_B = f_C = 0.25$. For the convenience of a direct comparison with the experimental results, we first examine the phase behavior of A(BC)$_2$B with similar compositions of $f_A = 0.50$, $f_B = 0.252$ (this value can be exactly divided into three species), and $f_C = 0.248$. In our calculations, we have checked that the small difference in compositions hardly influences the phase behavior. By varying the three interaction parameters, we search for different lamellar morphologies with random initial conditions by using the pseudospectral method of SCMFT. Three equilibrium morphologies of perpendicular or parallel lamellae in lamellae have been obtained, as shown in Figure 1. The domains with A, B, and C blocks as the majority components, are indicated by red, green, and blue, respectively. Here we denote the perpendicular morphology as $L_\perp$ (see Figure 1a) and the parallel morphologies as $L_k$ where $k$ indicates the number of internal B/C layers. There are two parallel morphologies of $L_3$ and $L_5$ shown in Figure 1b and d, respectively. In the $L_3$ structure, there is small amount of C components on the A/B interfaces which can be seen more clearly from the one-dimensional density plot in Figure 1c. The penetration of some C blocks through B domains to get into A domains should result in an energy penalty as the presence of the A/C interfacial energy. A significant A/C interfacial energy also exists in $L_\perp$. Compared with the two structures of $L_3$ and $L_\perp$, the A/C interfacial energy of $L_5$ is much lower because the C domains are well separated from A domains by B domains. According to this qualitative analysis, we can predict that $L_3$ and $L_\perp$ could become stable only when $\chi_{AC}$ is weak. To gain a systematic understanding on the relative stability of the three phases, it is

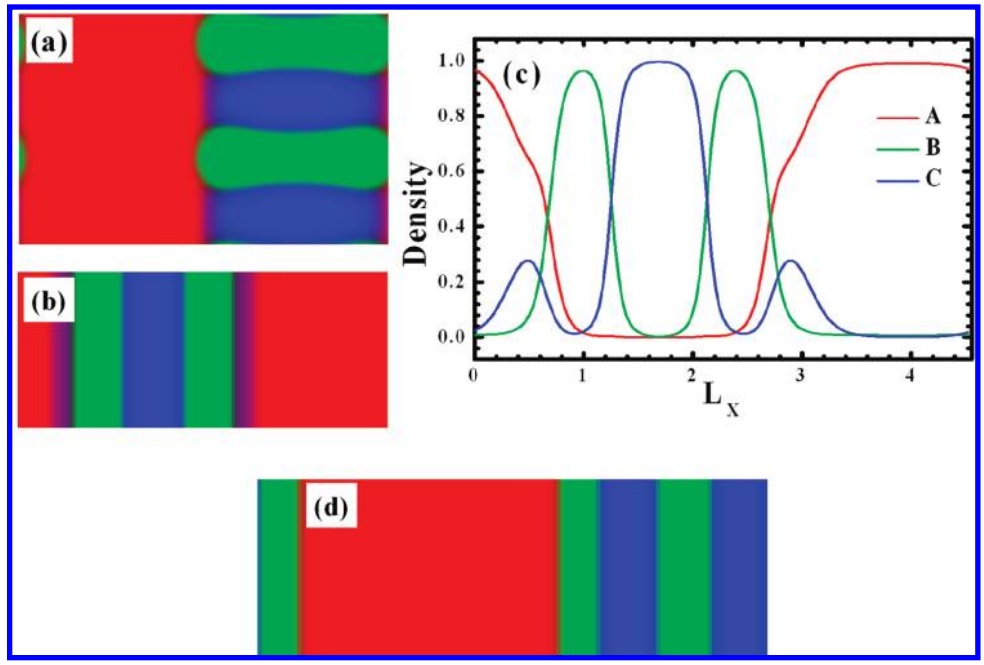


**Figure 1.** Typical density plots of hierarchical lamellar morphologies observed in the multiblock terpolymer of A(BC)$_2$B with fixed compositions of $f_A = 0.5$, $f_B = 0.252$, and $f_C = 0.25$. The perpendicular lamellae in lamellae are denoted as $L_\perp$, and the parallel lamellae in lamellae are denoted as $L_k$, where $k$ indicates the number of internal B/C layers. The colors of red, green, and blue indicate the domains where the largest component is A, B, and C, respectively. There are three hierarchical lamellar morphologies: $L_\perp$ (a), $L_3$ (b), and $L_5$ (d). The one-dimensional density profiles of $L_3$ are plotted in c.

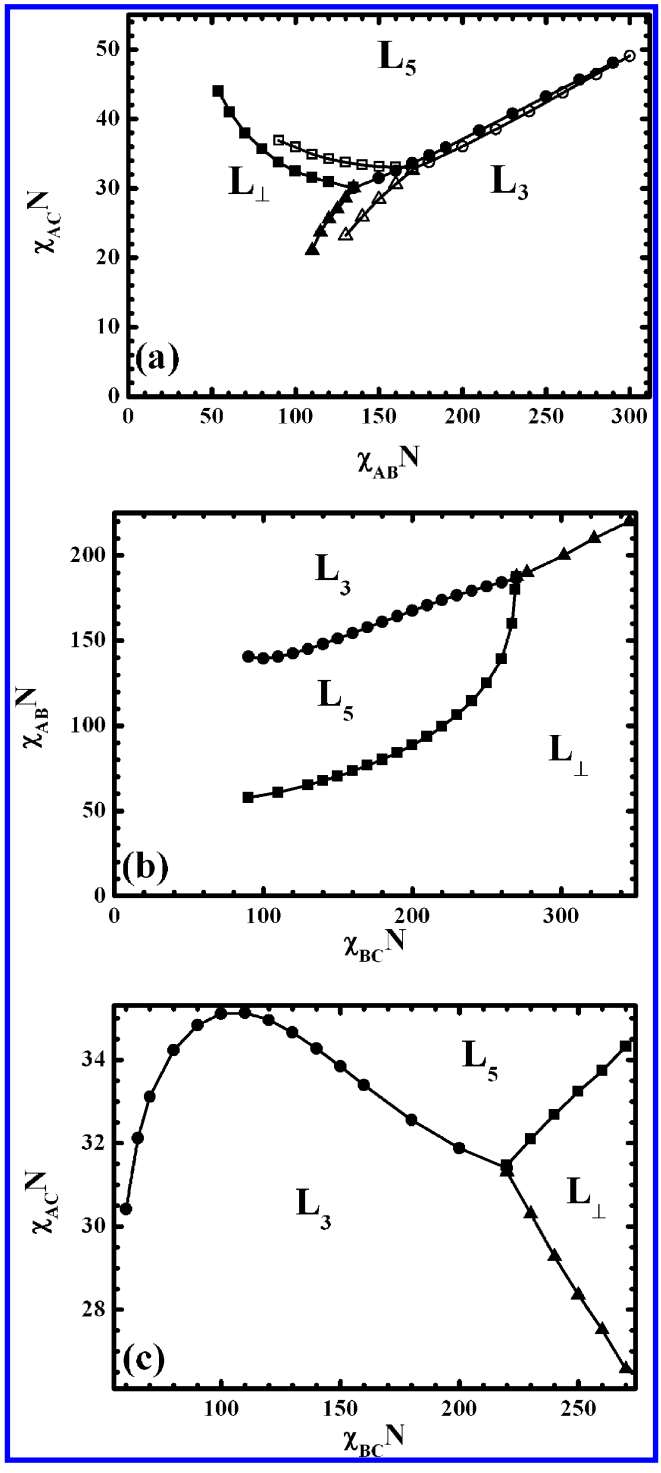


**Figure 2.** Two-dimensional phase diagrams about the terpolymer of $A(BC)_2B$ in Figure 1: (a) for fixed $\chi_{BC}N = 200$ (filled symbols) and $\chi_{BC}N = 250$ (unfilled symbols); (b) for fixed $\chi_{AC}N = 34$; and (c) for fixed $\chi_{AB}N = 150$. These symbols are the calculated points, and the connected lines are a guide for the eye.

necessary to calculate the phase diagram as a function of interaction parameters. Although the compositions are fixed, the phase diagram is still three-dimensional (3D) as it depends on the three interaction parameters of $\chi_{AB}N$, $\chi_{AC}N$, and $\chi_{BC}N$. The task of constructing a full 3D phase diagram is formidable. Therefore, we present different 2D cross sections of the 3D phase diagram by fixing one of the three parameters.

Three 2D phase diagrams for fixed $\chi_{BC}N = 200$, $\chi_{AC}N = 34$, and $\chi_{AB}N = 150$ are present in parts a, b, and c of Figure 2,

**TABLE 1: Numbers of Possible Configurational Paths of the Multiblock Terpolymers in Different Morphologies of Perpendicular or Parallel Lamellae in Lamellae[a]**

| terpolymers | $L_\perp$ | $L_3$ | $L_5$ | $L_7$ |
|---|---|---|---|---|
| $A(BC)_2B$ | 8 | 9 (4) | (6) | |
| $A(BC)_3$ | 16 | 13 (4) | 19 (8) | (10) |
| $A(BC)_3B$ | 29 | 21 (8) | 33 (17) | (20) |

[a] The numbers in brackets are counted without considering the penetration of C blocks through B domains to get onto the A/B interfaces.

respectively. In these phase diagrams the symbols present the calculated transition boundaries, whereas the connected lines are simply a guide for the eyes. The phase diagram of Figure 2a shows that $L_\perp$ and $L_3$ are stable only when $\chi_{AC}N$ is very weak, and $L_5$ becomes stable when $\chi_{AC}N$ increases. This is consistent with the analysis of the A/C interfacial energy. At the region of weak $\chi_{AC}N$, $L_\perp$ transfers to $L_3$ when $\chi_{AB}N$ is increased. The three order−order phase transition (OOT) lines join at a triple point of $(\chi_{AB}N,\ \chi_{AC}N) \approx (135.6,\ 30.2)$. It is known that the structure formation in the block copolymer self-assembly is determined by the delicate balance between the interfacial energy and the entropic energy. In the model multiblock terpolymer studied here, the entropic free energy can be divided into two contributions: the stretching energy of each block and the paths for the arrangements of these blocks in the corresponding domains.[20] The second part can be qualitatively described by the number of possible paths whose values are given in Table 1 for possible morphologies formed in $A(BC)_2B$, $A(BC)_3$, and $A(BC)_3B$.[19] When counting the possible paths of the parallel lamellar phases, we have to consider whether there is C-block penetration through B domains to get onto the A/B interfaces. The penetration significantly increases the possible paths. There are three main cases. In the first case, the penetration exists in the whole phase regions of the morphologies, like $L_3$ of $A(BC)_3$ and $A(BC)_3B$. The configurational paths always include those with the penetration (those values without brackets). In the second case opposite to the first one, the penetration is rare in the whole phase regions of the morphologies like $L_5$ of $A(BC)_2B$, and $L_7$ of $A(BC)_3$ and $A(BC)_3B$. For this case, only the nonpenetration paths are counted (shown in the brackets). In the third case, an intermediate between the former two cases, the penetration is strongly dependent on the interaction of $\chi_{AC}N$ and decreases as it increases. Schematic plots of the possible arrangements for the terpolymer of $A(BC)_2B$ in morphologies $L_\perp$, $L_3$, and $L_5$ are presented in Figure 3. Compared with the parallel lamellae formed in symmetric $A(BC)_nBA$ terpolymers, where the B/C-mid layers are softly confined between two large A layers in which the two ends have to be located, the confinement effect in those of $A(BC)_nB$ or $A(BC)_n$ becomes weaker as the end on the B (or C) block can go to any of B (or C) domains. Nevertheless, the number of possible paths is still one important factor on the relative stability among these morphologies. For the $A(BC)_2B$ terpolymer, the path number of $L_3$, decreasing from 9 to 4 when most of the C components are expelled away from the A/C interfaces by large $\chi_{AC}N$, is smaller than that of $L_5$ (6). So $L_5$ becomes stable for large $\chi_{AC}N$. Although $L_\perp$ has more configurational paths, the increased A/C interfacial energy destroys its stability. When $\chi_{AC}N$ is weak, the number of possible paths is respectively 8 and 9 for $L_\perp$ and $L_3$, and therefore their merit of the configurational paths relative to $L_5$ favors their stability. This point can be more directly seen from the data of free energy shown in Figure 4 for fixed $\chi_{AC}N = 34$. For the reason of clarity, Figure 4a shows the free energy

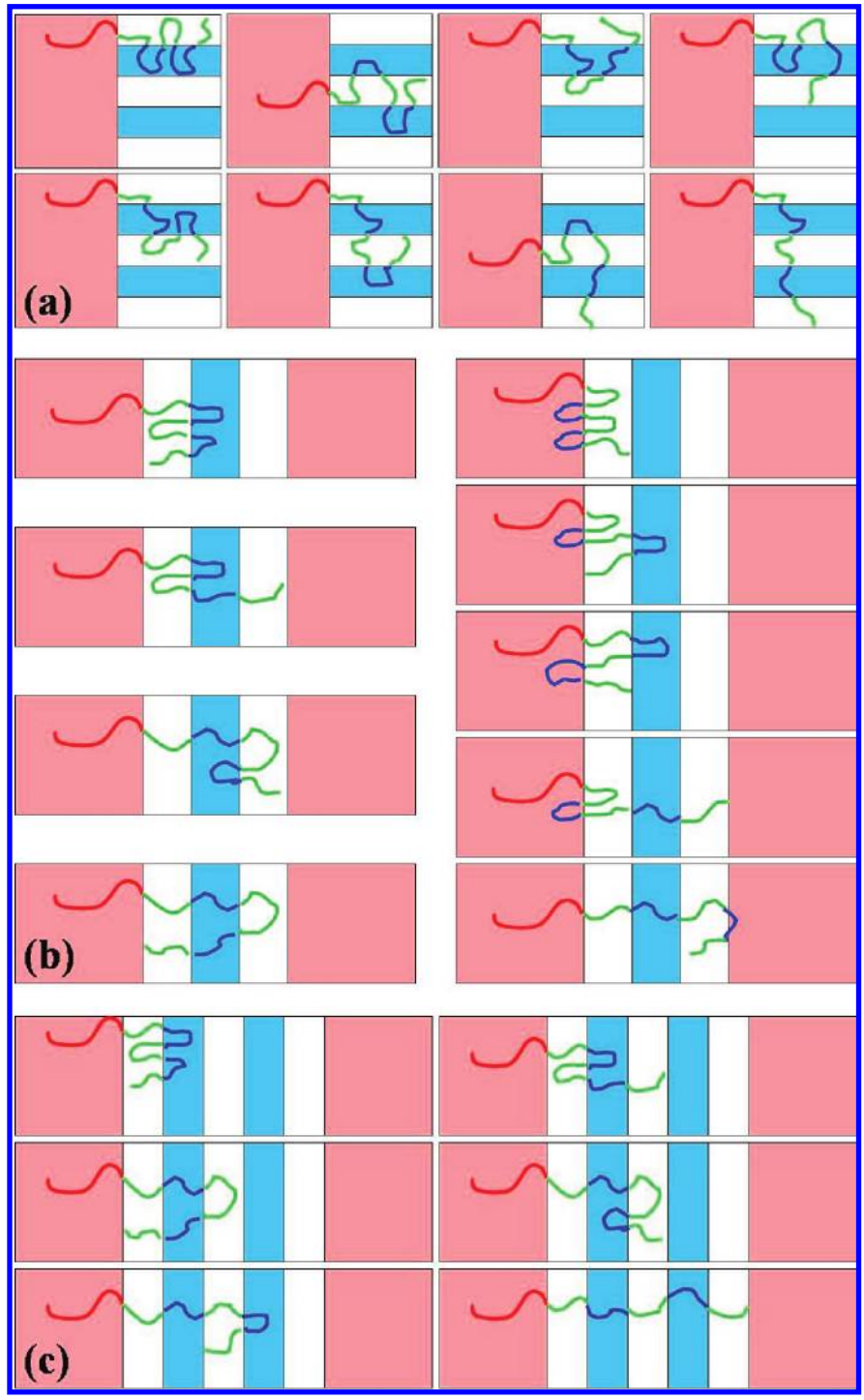


**Figure 3.** Schematic representation of the possible arrangements of the terpolymer, $A(BC)_2B$, in three morphologies of (a) $L_\perp$, (b) $L_3$, and (c) $L_5$.

difference defined as the free energy of a morphology subtracted by that of $L_\perp$, and Figure 4b and c show the entropic and internal energy contributions of free energy, respectively. The stable phase sequence is $L_\perp$, $L_5$, and $L_3$ for increasing $\chi_{AB}N$, and the two OOTs are indicated by the arrows at $\chi_{AB}N \approx 88.6$ and $\chi_{AB}N \approx 167.6$. The plot of entropic contributions clearly suggests that $L_3$ has the most favorable value and $L_5$ has the highest value. On the other hand, the situation of the internal energy is reversed. So the stability of $L_\perp$ and $L_3$ relative to $L_5$ is attributed to their favorable entropic contribution from the configurational paths and the minor A/C interfacial energy because of weak $\chi_{AC}N$. The stability of $L_3$ relative to $L_\perp$ for high $\chi_{AB}N$ can be explained by the factor that the C components on A/B interfaces are favorable to reduce the A/B interfacial energy induced by increased $\chi_{AB}N$. The reverse case of the OOT from $L_3$ to $L_\perp$ with decreasing $\chi_{AB}N$ can be explained by the entropic contribution from the stretching energy of each block. In $L_3$, the confinement on the B/C domains imposed by two thick A domains results in the penalty of stretching energy of B/C blocks. However, the B/C domains in $L_\perp$ can adjust their periods more freely along their normal directions to minimize the stretching energy. When decreasing $\chi_{AB}N$, the factor of stretching energy becomes more dominant and drives the OOT from $L_3$ to $L_\perp$.

The period of the morphologies is closely related to the stretching of the polymer chains. In Figure 5, the period of the

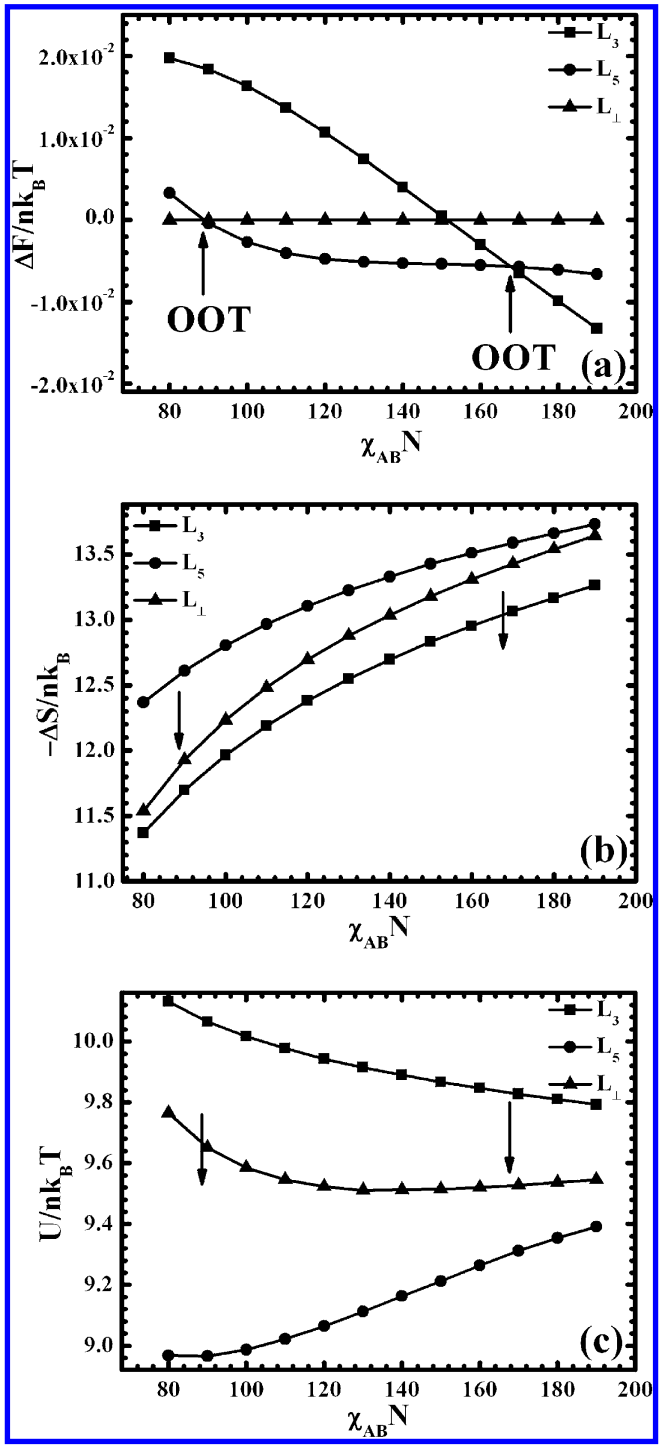


**Figure 4.** (a) Free energy difference, subtracted by the value of free energy of $L_\perp$, as a function of $\chi_{AB}N$ with fixed $\chi_{AC}N = 34$ and $\chi_{BC}N = 200$, and therefore $\Delta F/nk_BT$ of $L_\perp$ is always zero; (b) entropic and (c) internal part of free energy for the three phases. Two order−order transitions (OOT) are indicated by two arrows.

three phases is present for two cases: (a) as a function of $\chi_{AB}N$ for fixed $\chi_{AC}N = 34$ and $\chi_{BC}N = 200$; (b) as a function of $\chi_{BC}N$ for fixed $\chi_{AC}N = 34$ and $\chi_{AB}N = 150$. For parallel phases of $L_3$ and $L_5$, their periods increase as $\chi_{AB}N$ or $\chi_{BC}N$ increases because the chains are stretched to reduce the corresponding interfacial energy. However, for the perpendicular phase of $L_\perp$, there are two periods: $L_{\perp,x}$ along the normal direction of the major lamellae and $L_{\perp,y}$ along that of the B/C sublayers. The mechanism that $L_{\perp,x}$ increases as $\chi_{AB}N$ increases is similar to that of the periods of $L_3$ or $L_5$. However, for $L_{\perp,y}$, the changing magnitude is less than 2% because the perpendicularly arranged B/C sublayers are much less influenced by the A/B interfaces. The small change of $L_{\perp,y}$ is induced by the shape adjustment of the curved A/B and A/C interfaces. Similarly, $L_{\perp,x}$ does not change appreciably like $L_{\perp,y}$ does when $\chi_{BC}N$ is increased in Figure 5b The results of period reveal that $L_\perp$ has more freedom to minimize the stretching energy than the parallel phases.

To demonstrate the influence of $\chi_{BC}N$ on the 2D phase diagram in Figure 2a, the phase boundaries between the three phases $L_3$, $L_5$, and $L_\perp$ for $\chi_{BC}N = 250$ (unfilled symbols) are present as a comparison of $\chi_{BC}N = 200$ (filled symbols). The triple point, shifting from ($\chi_{AB}N$, $\chi_{AC}N$) ≈ (135.6, 30.2) to (170.0, 32.8), suggests that larger $\chi_{BC}N$ favors the stability of $L_\perp$. The phase region of $L_\perp$ expands toward a larger $\chi_{AB}N$ and $\chi_{AC}N$. However, the shift along $\chi_{AC}N$ induced by the increment of 50 in $\chi_{BC}N$ is very small. The 2D phase diagram with respect to $\chi_{BC}N$ and $\chi_{AB}N$ for fixed $\chi_{AC}N = 34$ in Figure 2b and that with respect to $\chi_{BC}N$ and $\chi_{AC}N$ for fixed $\chi_{AB}N = 150$ in Figure 2c show a more systematic influence of each interaction. Combining these three phase diagrams, it can be concluded that $L_\perp$ is stable in the case of $\chi_{AC} \ll \chi_{AB} < \chi_{BC}$. This is consistent with the observation of the experiments.[27]

Previous studies suggested that the phase diagram is strongly determined by the number of B or C blocks.[20] As a comparison, we also studied the phase behaviors of $A(BC)_3$ and $A(BC)_3B$ with fixed $f_A = 0.50$, $f_B = 0.25$, $f_C = 0.25$, and $\chi_{BC}N = 200$. The corresponding 2D phase diagrams are presented in Figure 6. The choice of high $\chi_{BC}N$ ensures the presence of the phase region of $L_\perp$. After adding one C block or one repeating unit of B and C blocks, the parallel lamellar phase of $L_7$ with seven internal B/C layers becomes a stable phase in both Figure 6b and c. As the number of B/C layers increases, less C component is observed on the A/B interfaces (more discussion below). Compared with $A(BC)_3$, the phase region of $L_7$ in the phase diagram of $A(BC)_3B$ expands toward the region of lower $\chi_{AB}N$ and $\chi_{AC}N$. The increased stability of $L_7$ relative to $L_5$ can be explained by the change of the numbers of their possible paths (see Table 1). The common features among the two phase diagrams as well as that of Figure 2a are that $L_\perp$ and $L_3$ appear as stable phases in the similar phase region of weak $\chi_{AC}N$. The SST study by Subbotin et al. has predicted that $L_\perp$ expands toward the phase region of larger $\chi_{AC}N$ when increasing the repeating number of $n$.[36] However, from the triple points of $A(BC)_2B$, $A(BC)_3$, and $A(BC)_3B$, ($\chi_{AB}N$, $\chi_{AC}N$) = (135.6, 30.2), (112.1, 31.6), and (130.1, 21.8), this trend is not observed. The contradiction between the SST results and that of our SCMFT can be accounted for by two main reasons. One reason is that the interactions used in this work do not belong to the strong-segregation case. In most cases, the value of $\chi_{AC}N$ is small, and even for the case of $\chi_{BC}N = 200$ in $A(BC)_2B$, the segregation between B and C is not strong because the effective interaction between each pair of B and C blocks is $\chi_{BC}(N_B/3 + N_C/2) \approx 41.7$. The second reason is that there is some C component on the A/B interfaces when $\chi_{AC}N$ is small in the parallel phase like $L_3$. The penetration of C block to get into A domains is helpful to stabilize the parallel morphology.

In Figure 5, we have shown the period, as a function of $\chi_{AB}N$ and $\chi_{BC}N$, of different morphologies formed in $A(BC)_2B$. To gain an understanding on the influence of $\chi_{AC}N$ on the structure transformation, we plot the period, as a function of $\chi_{AC}N$ for fixed $\chi_{AB}N = 130$ and $\chi_{BC}N = 200$, of the parallel morphologies of $A(BC)_3B$ in Figure 7a. From bottom to top, the periods are for $L_3$, $L_5$, and $L_7$, respectively. For $L_3$, the period is a monotonically increasing function of $\chi_{AC}$. However, for $L_5$ and

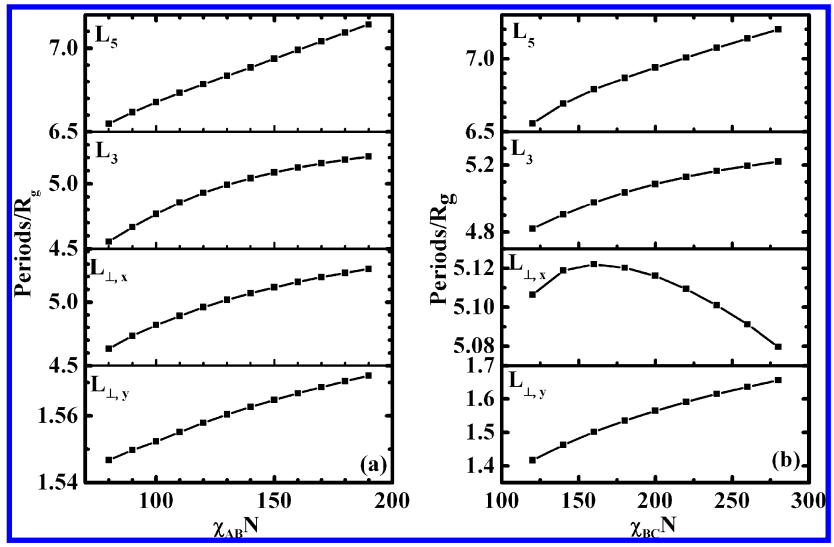


**Figure 5.** Period of different morphologies (a) as a function of $\chi_{AB}N$ for fixed $\chi_{AC}N = 34$ and $\chi_{BC}N = 200$ and (b) as a function of $\chi_{BC}N$ for fixed $\chi_{AC}N = 34$ and $\chi_{AB}N = 150$. The two periods of $L_\perp$ are denoted as $L_{\perp,x}$ and $L_{\perp,y}$, respectively.

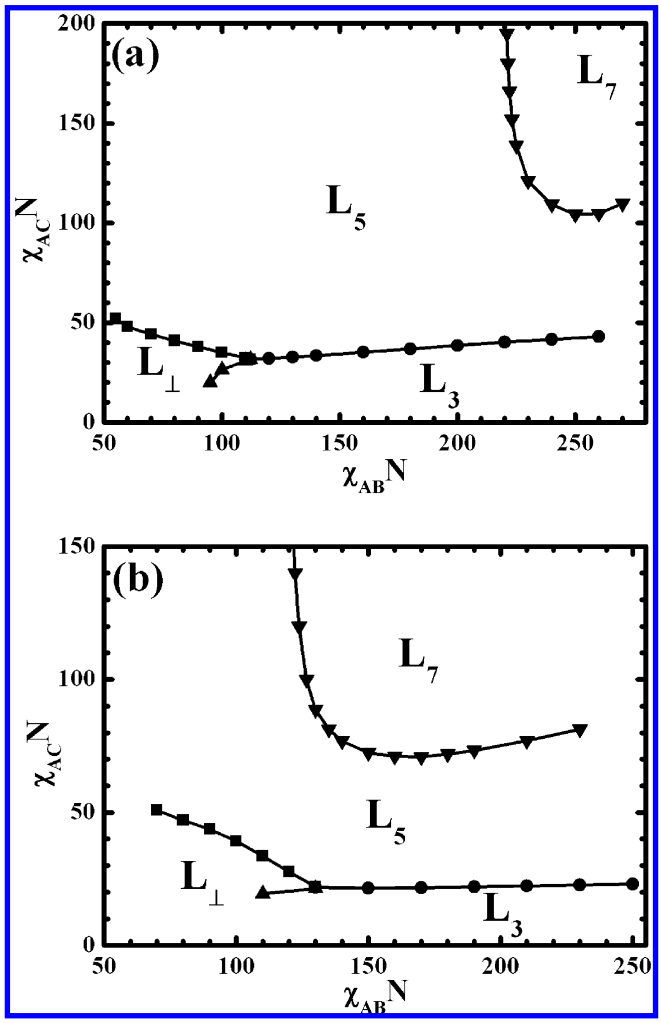


**Figure 6.** 2D phase diagrams with respect to $\chi_{AB}N$ and $\chi_{AC}N$ for multiblock terpolymers of (a) $A(BC)_3$ and (b) $A(BC)_3B$ with fixed $\chi_{BC}N = 200$.

$L_7$, the periods do not change monotonically. From the density distributions of $L_3$ in d, we find that there is always a C component on the A/B interfaces even for strong $\chi_{AC}N$, and the quantity of C is large. In this sense, the number of internal B/C layers in $L_3$ is not three, but five. Although it makes more sense to rename this morphology according to CBCBC layer sequence (like inverted $L_5$), here we still use $L_3$ to denote it to be consistent with the other morphologies. For $L_5$, the quantity of the C component on the A/B interfaces becomes much less and decreases fast as $\chi_{AC}N$ increases, and therefore the decreasing of C component reduces its period. The ability to adjust the quantity of C makes $L_5$ more stable than $L_3$ when $\chi_{AC}N \gtrsim 21.8$. However, when $\chi_{AC}N \gtrsim 88.7$, most of the C component on the A/B interfaces has gone, and the period of $L_5$ does not change appreciably (only slightly increasing) as $\chi_{AC}N$ increases. Only those configurational paths without the penetration contribute to the free energy, and therefore the number of paths becomes 17 which is smaller than that of $L_7$. This is why $L_5$ transfers to $L_7$ at $\chi_{AC}N \approx 88.7$. In $L_7$ with $\chi_{AC}N = 80$, there is no obvious density peak of the C component. In conclusion, the C component, formed by the penetrated C blocks through the B domains into the A domains, plays an important role in the adjustment of the relative stability among the parallel phases of $L_k$.

For $A(BC)_3$, the 2D phase diagram with respect to $\chi_{BC}N$ and $\chi_{AC}N$ for fixed $\chi_{AB}N = 100$ and $\chi_{AB}N = 150$ has been given in Figure 7 of ref 29. However, in their phase diagram, only the phase boundary between $L_\perp$ and $L_5$ is determined. When their phase boundary is extended into the region of smaller or larger $\chi_{AC}N$, $L_3$ and $L_7$ will appear as the stable phase.

The above results indicate that the presence of $L_\perp$ is rather insensitive to the number of short B/C blocks. Does the perpendicular lamellar-in-lamellar phase also exist in the ABC linear terpolymer which is the limit case of $A(BC)_n$ with $n = 1$? In the frustrated ABC terpolymers, many decorated phases, such as cylinders in lamellae, spheres in lamellae, spheres on cylinders, and rings on cylinders, have been observed.[31] However, to the best of our knowledge, the $L_\perp$ phase has not been observed with the linear ABC terpolymer. Here we consider the terpolymers of type II frustration with $\chi_{AC}N \ll \chi_{AB}N = \chi_{BC}N$. The 2D phase diagram of fixed compositions $f_A = 0.5$ and $f_B = f_C = 0.25$ is shown in Figure 8. As there are only two candidate stable phases of $L_\perp$ and $L_3$ (also named as core−shell lamellae), the phase diagram composes of one transition boundary dividing the two phase regions. It is seen that the transition boundary is almost linear, and $L_\perp$ can be stable only when $\chi_{AC}N$ is at least one order weaker than $\chi_{AB}N = \chi_{BC}N$. This is why $L_\perp$ was not observed by Zheng and Wang.[31]

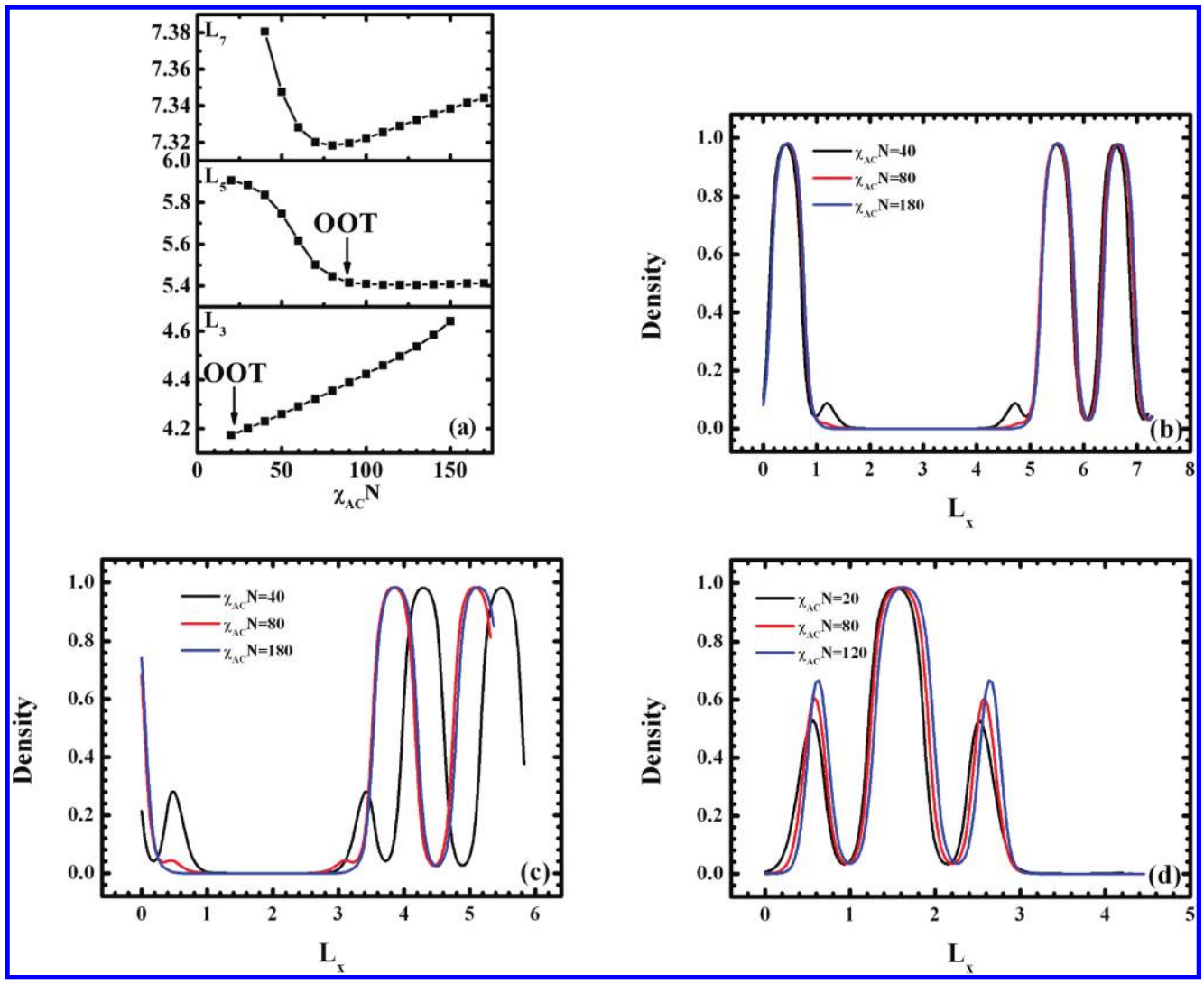


**Figure 7.** (a) Periods of $L_3$, $L_5$, and $L_7$, formed in the terpolymer A(BC)$_3$B, as a function of $\chi_{AC}N$ for fixed $\chi_{AB}N = 130$ and $\chi_{BC}N = 200$. Two OOTs are indicated by the arrows. b, c, and d are the density plots of C component in $L_7$, $L_5$, and $L_3$, respectively.

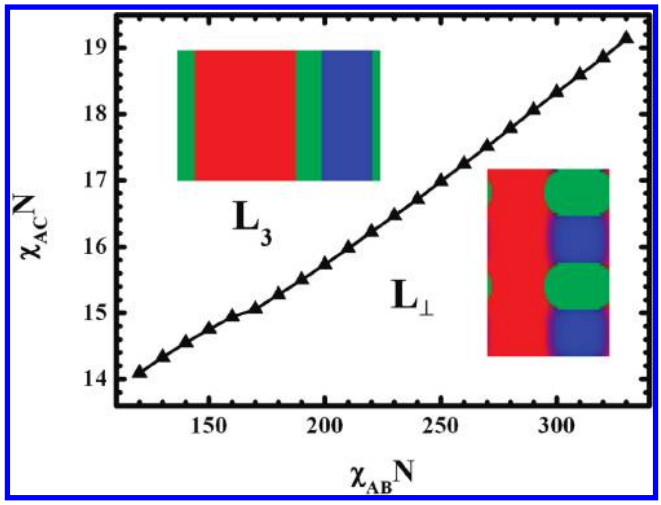


**Figure 8.** 2D phase diagram of the ABC linear terpolymer with fixed $\chi_{AB}N = \chi_{BC}N$ and fixed compositions $f_A = 0.5$ and $f_B = f_C = 0.25$. The density plots of $L_\perp$ and $L_3$ are inserted.

## IV. Conclusions

In conclusion, we have studied the formation of hierarchical perpendicular or parallel lamellae of multiblock terpolymers of the type of A(BC)$_2$B, A(BC)$_3$, and A(BC)$_3$B. First of all, we have constructed the 2D phase diagrams by fixing one of the three interaction parameters for the terpolymer of A(BC)$_2$B with fixed compositions. For this terpolymer, three equilibrium phases, the $L_\perp$, $L_3$, and $L_5$ phases, are observed. For $L_3$, some C blocks penetrate the B domains into A domains, and they play a significant role to stabilize $L_3$ phase by reducing the A/B interfacial energy for weak $\chi_{AC}N$ and high $\chi_{AB}N$. Our results suggest that $L_\perp$ is stable when the three interactions satisfy the situations of $\chi_{AC} \ll \chi_{AB} < \chi_{BC}$. The stability of $L_\perp$ relative to the other two phases in this region can be well-interpreted by the delicate balance between the two contributions of interfacial energy and entropic energy in free energy. Our conclusion is consistent with the experimental observations. Then we calculated the phase diagrams of A(BC)$_3$ and A(BC)$_3$B with $f_A = 0.5$, $f_B = f_C = 0.25$, and $\chi_{BC}N = 200$. For the two terpolymers, the parallel lamellar phase of $L_7$ with seven internal B/C layers becomes a stable phase, and its phase region expands into smaller $\chi_{AC}N$ and $\chi_{AB}N$. Finally, we studied the relative stability of $L_\perp$ and $L_3$ in the ABC linear terpolymers with type II frustration by fixing $\chi_{AB}N = \chi_{BC}N$. $L_\perp$ can still exist as the stable phase, but in the phase region with a much weaker $\chi_{AC}N$ than those of other terpolymers. By comparing the phase diagrams among these terpolymers, we find that the presence of the

perpendicular phase of $L_\perp$ is a generic feature of linear multiblock terpolymers.

**Acknowledgment.** This work was supported by the National Natural Science Foundation of China (Grants 20974026, 20704010, 20625413). W.L. gratefully acknowledges support from the Shanghai Pujiang Program (Program No. 08PJ1402000), the Shanghai Educational Development Foundation (Program No. 2008CG02), and the Scientific Research Foundation for the Returned Overseas Chinese Scholars, State Education Ministry.

## References and Notes

(1) Park, M.; Harrison, C.; Chaikin, P. M.; Register, R. A.; Adamson, D. H. *Science* **1997**, *276*, 1401.
(2) Thurn-Albrecht, T.; Schotter, J.; Kastle, C. A.; Emley, N.; Shibauchi, T.; Krusin-Elbaum, L.; Guarini, K.; Black, C. T.; Tuominen, M. T.; Russell, T. P. *Science* **2000**, *290*, 2126.
(3) Cheng, J. Y.; Ross, C. A.; Chan, V. Z. H.; Thomas, E. L.; Lammertink, R. G. H.; Vancso, G. J. *Adv. Mater.* **2001**, *13*, 1174.
(4) Black, C. T.; Guarini, K. W.; Milkove, K. R.; Baker, S. M.; Russell, T. P.; Tuominen, M. T. *Appl. Phys. Lett.* **2001**, *79*, 409.
(5) Matsen, M. W.; Schick, M. *Phys. Rev. Lett.* **1994**, *72*, 2660.
(6) Matsen, M. W. *J. Phys.: Condens. Matter* **2002**, *14*, R21.
(7) Tyler, C. A.; Morse, D. C. *Phys. Rev. Lett.* **2005**, *94*, 208302.
(8) Tyler, C. A.; Qin, J.; Bates, F. S.; Morse, D. C. *Macromolecules* **2007**, *40*, 4654.
(9) Guo, Z.; Zhang, G.; Qiu, F.; Zhang, H.; Yang, Y.; Shi, A.-C. *Phys. Rev. Lett.* **2008**, *101*, 028301.
(10) Bohbot-Raviv, Y.; Wang, Z. G. *Phys. Rev. Lett.* **2000**, *86*, 3428.
(11) Gemma, T.; Hatano, A.; Dotera, T. *Macromolecules* **2002**, *35*, 3225.
(12) Matsushita, Y. *Macromolecules* **2007**, *40*, 771.
(13) Zhang, G. J.; Qiu, F.; Zhang, H. D.; Yang, Y. L.; Shi, A. C. *Macromolecules* **2010**, *43*, 2981.
(14) Li, W. H.; Xu, Y. C.; Zhang, G. J.; Qiu, F.; Yang, Y. L.; Shi, A. C. *J. Chem. Phys.* **2010**, *133*, 064904.
(15) Ruokolainen, J.; Makinen, R.; Serimaa, R.; ten Brinke, G.; Ikkala, O. *Science* **1998**, *280*, 557.
(16) Ikkala, O.; ten Brinke, G. *Science* **2002**, *295*, 2407.
(17) Ruokolainen, J.; ten Brinke, G.; Ikkala, O. *Adv. Mater.* **1999**, *11*, 777.
(18) Nagata, Y.; Masuda, J.; Noro, A.; Cho, D. Y.; Takano, A.; Matsushita, Y. *Macromolecules* **2005**, *38*, 10220.
(19) Masuda, J.; Takano, A.; Nagata, Y.; Noro, A.; Matsushita, Y. *Phys. Rev. Lett.* **2006**, *97*, 098301.
(20) Li, W. H.; Shi, A. C. *Macromolecules* **2009**, *42*, 811.
(21) Klymko, T.; Markov, V.; Subbotin, A.; ten Brinke, G. *Soft Matter* **2009**, *5*, 98.
(22) Nap, R.; Sushko, N.; Erukhimovich, I.; ten Brinke, G. *Macromolecules* **2006**, *39*, 6765.
(23) Zhang, L. S.; Lin, J. P. *Macromolecules* **2009**, *42*, 1410.
(24) Kriksin, Y. A.; Erukhimovich, I. Y.; Smirnova, Y. G.; Khalatur, P. G.; ten Brinke, G. *J. Chem. Phys.* **2009**, *130*, 204901.
(25) Subbotin, A.; Klymko, T.; ten Brinke, G. *Macromolecules* **2007**, *40*, 2915.
(26) Klymko, T.; Subbotin, A.; ten Brinke, G. *J. Chem. Phys.* **2008**, *129*, 114902.
(27) Fleury, G.; Bates, F. S. *Macromolecules* **2009**, *42*, 1691.
(28) Fleury, G.; Bates, F. S. *Macromolecules* **2009**, *42*, 3598.
(29) Wang, L. Q.; Lin, J. P.; Zhang, L. S. *Macromolecules* **2010**, *43*, 1602.
(30) Bailey, T. S. Morphological behavior spanning the symmetric AB and ABC block copolymer states. Thesis, University of Minnesota, 2001.
(31) Zheng, W.; Wang, Z. G. *Macromolecules* **1995**, *28*, 7215.
(32) Shi, A. C. *Development in Block Copolymer Science and Technology*; Hamley, I. W., Ed.; Wiley: New York, 2004.
(33) Fredrickson, G. H. *The Equilibrium Theory of Inhomogeneous Polymers*; Oxford University Press: Oxford, U.K., 2006.
(34) Tzeremes, G.; Rasmussen, K. Ø.; Lookman, T.; Saxena, A. *Phys. Rev. E* **2002**, *65*, 041806.
(35) Rasmussen, K. Ø.; Kalosakas, G. J. *J. Polym. Sci., Part B: Polym. Phys.* **2002**, *40*, 1777.
(36) Subbotin, A.; Markov, V.; ten Brinke, G. *J. Phys. Chem. B* **2010**, *114*, 5250.

JP1068335